RESEARCH ARTICLES

SLEEP RESEARCH

Changes in the composition of brain interstitial ions control the sleep-wake cycle

Fengfei Ding,[1,2]* John O'Donnell,[1]* Qiwu Xu,[1] Ning Kang,[1] Nanna Goldman,[1] Maiken Nedergaard[1,3]†

Wakefulness is driven by the widespread release of neuromodulators by the ascending arousal system. Yet, it is unclear how these substances orchestrate state-dependent, global changes in neuronal activity. Here, we show that neuromodulators induce increases in the extracellular K^+ concentration ($[K^+]_e$) in cortical slices electrically silenced by tetrodotoxin. In vivo, arousal was linked to AMPA receptor–independent elevations of $[K^+]_e$ concomitant with decreases in $[Ca^{2+}]_e$, $[Mg^{2+}]_e$, $[H^+]_e$, and the extracellular volume. Opposite, natural sleep and anesthesia reduced $[K^+]_e$ while increasing $[Ca^{2+}]_e$, $[Mg^{2+}]_e$, and $[H^+]_e$ as well as the extracellular volume. Local cortical activity of sleeping mice could be readily converted to the stereotypical electroencephalography pattern of wakefulness by simply imposing a change in the extracellular ion composition. Thus, extracellular ions control the state-dependent patterns of neural activity.

Wakefulness and sleep represent two fundamentally different behavioral states (*1*). While awake, we are responsive to our surroundings, integrate sensory input, recall memories, and make decisions, whereas contact with the outside world is limited during sleep. These two states of brain activity show characteristic patterns of cortical electroencephalography (EEG), gene expression, and metabolic signature (*2*, *3*). The concerted release of neuromodulators—including norepinephrine, acetylcholine, histamine, dopamine, and orexin—mediates arousal (*4*). All of these neuromodulators individually alter the membrane properties, spiking activity, and intracellular signaling pathways of subpopulations of neurons and glia (*5*), but how they implement the striking stereotypic patterns of EEG activity characterizing wakefulness versus sleep is not understood (*6*).

Neuronal excitability can be modulated by changes in the composition of extracellular ions. For example, moderate elevations of $[K^+]$ in the bath solution (1 to 2 mM) increase spontaneous and evoked excitatory activity in hippocampal slices, and more robust elevations (2 to 5 mM) trigger seizure-like activity (*7*). Lowering extracellular Ca^{2+} ($[Ca^{2+}]_e$) and extracellular Mg^{2+} ($[Mg^{2+}]_e$) also potently alters excitability (*7*).

[1]Center for Translational Neuromedicine, University of Rochester Medical Center, Rochester, NY 14642, USA. [2]Department of Neurology, Tongji Hospital, Tongji Medical College, Huazhong University of Science and Technology, Wuhan 430030, China. [3]Center for Basic and Translational Neuroscience, Faculty of Health and Medical Sciences, University of Copenhagen, Copenhagen 2200, Denmark. *These authors contributed equally to this work. †Corresponding author: Email: nedergaard@urmc.rochester.edu

Neuromodulators increase extracellular K^+ independently of synaptic activity

It is not known whether the changes in extracellular ion concentrations that occur during the natural sleep-wake cycle (*8*) are primary or secondary to alterations in electrical activity. In fact, the changes in extracellular ions that accompany behavioral states would be considered by most to be a consequence of different patterns of neuronal activity. However, ion transport is regulated by catecholamines outside the central nervous system (CNS) (*5*). We asked whether neuromodulators also regulate ion transport in the CNS and thereby the concentration of extracellular ions. We first recorded extracellular K^+ concentration ($[K^+]_e$) in cortical slices prepared from adult mice using K^+-sensitive microelectrodes (K^+-ISMs). Superfusion of a cocktail of neuromodulators at a concentration comparable with previous slice studies containing norepinephrine, acetylcholine, dopamine, orexin, and histamine triggered a rapid increase in $[K^+]_e$, averaging 0.43 ± 0.07 mM. Surprisingly, blocking neuronal activity by addition of tetrodotoxin (TTX) (1 μM) neither altered basal $[K^+]_e$ nor significantly suppressed the neuromodulator cocktail–induced $[K^+]_e$ increase, despite completely blocking spontaneous and evoked activity (Fig. 1). As a positive control, we inhibited energy metabolism by short-lasting exposure to the glycolytic inhibitor iodoacetate (10 min, 3.5 mM), triggering an abrupt increase in $[K^+]_e$, which partly recovered during washout (Fig. 1F). As expected, TTX suppressed the increase in $[K^+]_e$ induced by inhibition of glycolysis (*9*). The insensitivity of neuromodulator-induced $[K^+]_e$ elevations to TTX raises the question as to whether the concerted release of neuromodulators during arousal and wakefulness also drives an increase in $[K^+]_e$ in vivo, and if so, whether this elevation is upstream of excitatory transmission or merely secondary to changes in local neuronal activity.

Wakefulness triggers an increase in extracellular K^+ that is independent of AMPA receptors

We next measured state-dependent changes in extracellular ion concentrations in vivo (fig. S2A). All recordings were collected between zeitgeber times (ZT) 4 and 8 (ZT times are based on a 24-hour diurnal cycle standardized so that ZT0 is the beginning of the sleep period and ZT12 is the beginning of the awake period). Sleep was defined as periods with high electrocorticography (ECoG) delta activity and low electromyography (EMG) activity relative to periods when animals were awake. Starting from sleep, $[K^+]_e$ rose rapidly by 0.40 ± 0.05 mM (Fig. 2, A and B) as animals awoke, before returning to baseline as animals fell back asleep. These transitions occurred quickly, with increases peaking within 1.3 ± 0.02 s (range 0.1 to 8.6 s, n = 27 transitions), whereas the transition back to sleep was substantially slower and more variable, 13.9 ± 2.7 s [range 1.8 to 45.9 s, $t(55) = 3.22$, $P = 0.002$].

We next investigated the effect of isoflurane anesthesia on $[K^+]_e$ and collected recordings during the animals' natural wake period (ZT16 to ZT20). After obtaining a stable awake $[K^+]_e$ baseline, 2% isoflurane was administered, which consistently triggered a sharp decrease in $[K^+]_e$ of 0.37 ± 0.06 mM (Fig. 2C). This decrease in $[K^+]_e$ remained stable throughout isoflurane administration and recovered to pre-anesthesia awake levels over 148 ± 41 s after cessation of anesthesia (n = 9 animals). Both the shift into and recovery from anesthesia mirrored changes in ECoG and EMG activity (Fig. 2C).

To critically evaluate the stability of state-dependent ion shifts, microdialysis samples of the extracellular fluid were collected in freely behaving, unrestrained mice. We used the no-net flux paradigm to estimate $[K^+]_e$, with five samples collected over several hours in which the $[K^+]$ in artificial cerebrospinal fluid (ACSF) was stepwise altered (Fig. 2D). Estimates of $[K^+]_e$ were comparable with those recorded with K^+-ISMs in the cortex, 4.00 ± 0.17 mM versus 4.16 ± 0.09 mM in awake mice [$t(44) = 0.903$, $P = 0.371$, Student's t test]. Microdialysis also showed a significant reduction in $[K^+]_e$ during sleep and isoflurane periods, with values decreasing to 3.44 ± 0.11 mM in sleep and 3.26 ± 0.12 mM in isoflurane (Fig. 2D).

To test whether state-dependent $[K^+]_e$ shifts are the result of changes in excitatory activity in vivo, we applied the AMPA receptor antagonist 6-cyano-7-nitroquinoxaline-2,3-dione (CNQX) (200 μM). Although CNQX potently and rapidly

suppressed the ECoG power of awake mice, only a transient and short-lasting (<10 min) decrease in $[K^+]_e$ was observed, with $[K^+]_e$ returning to pre-CNQX concentrations despite continued suppression of synaptic activity (fig. S2, B, C, and F). Subsequent administration of isoflurane in the presence of CNQX decreased $[K^+]_e$ by 0.26 ± 0.02 mM (fig. S2C). Thus, regulation of $[K^+]_e$ is dependent on state-modulation and not a direct measure of local glutamatergic activity. State-dependent transitions in brain activity are also linked to changes in the extracellular space volume (*10*). Because the Na^+- and K^+-dependent adenosine triphosphatase (Na^+/K^+-ATPase) is the chief regulator of both $[K^+]_e$ and cell volume (*7*), we asked whether the decreased $[K^+]_e$ in response to isoflurane anesthesia is linked to expanded extracellular space. Despite markedly reducing ECoG power throughout recordings, CNQX neither changed awake extracellular space nor inhibited isoflurane-induced expansion (fig. S2E). This indicates that local synaptic transmission (ECoG power) is not the primary determinant of state-dependent changes of either $[K^+]_e$ or the extracellular space volume.

Together, cortical recordings of $[K^+]_e$ as well as sampling of the extracellular fluid by means of microdialysis showed consistent decreases in $[K^+]_e$ as animals transitioned from the awake state to sleep. Blocking local synaptic transmission with CNQX did not affect state-dependent changes in $[K^+]_e$ (Fig. 2E).

Extracellular Ca^{2+} decreases during wakefulness

Are cortical extracellular Ca^{2+} concentrations also regulated by the sleep-wake cycle? Opposite to the rise in $[K^+]_e$, $[Ca^{2+}]_e$ consistently decreased 0.13 ± 0.02 mM as mice transitioned from sleep to awake states and, conversely, increased by 0.11 ± 0.01 mM as the mice returned to sleep (Fig. 3, A and B). These state-dependent $[Ca^{2+}]_e$ shifts were slow compared with those of $[K^+]_e$, with sleep-to-awake transitions taking 51.5 ± 8.8 s [$[Ca^{2+}]_e$, 4.5 to 156.0 s, Student's *t* test; versus $[K^+]_e$, $t(20) = 5.379$, $P < 0.0001$] and awake-to-sleep occurring over 63.3 ± 8.9 s [$[Ca^{2+}]_e$, 19.3 to 116.1 s, Student's *t* test; versus $[K^+]_e$, $t(16) = 6.696$, $P < 0.0001$]. Isoflurane administered to awake mice drove a slow increase in $[Ca^{2+}]_e$ throughout the duration of anesthesia, with levels rising by 0.26 ± 0.02 mM (Fig. 3C). This rise in $[Ca^{2+}]_e$ continued throughout and past the cessation of anesthesia, peaking at 1.2 ± 1.6 min (−6.2 to 12.4 min, $n = 11$ animals) and taking 22.6 ± 4.8 min (4.3 to 49.2 min, $n = 10$ animals) to recover.

Microdialysis was used to assess the stability of state-dependent $[Ca^{2+}]_e$ shifts by using the no-net flux method. Because of the slow time-course of $[Ca^{2+}]_e$ transitions and short awakenings associated with sample collection, we pooled sleep and awake samples and compared them with isoflurane, finding that $[Ca^{2+}]_e$ increases by 0.25 ± 0.08 mM under isoflurane anesthesia (Fig. 3D), which is comparable with in vivo $[Ca^{2+}]_e$ isoflurane recordings (Fig. 3E).

CNQX suppressed ECoG power by >60% but did not alter awake $[Ca^{2+}]_e$ or isoflurane-induced $[Ca^{2+}]_e$ increases (Fig. 3E), indicating that local glutamatergic activity did not control the shifts in $[Ca^{2+}]_e$. Together, all shifts from awake to isoflurane-anesthetized states showed surprising consistency (Fig. 3E). However, state-dependent changes in $[Ca^{2+}]_e$ could be secondary to shifts in $[K^+]_e$. We therefore increased $[K^+]_e$ in the ACSF covering the cranial window from 2.8 to 4.5 mM, increasing $[K^+]_e$ 200 μm below the pial surface by 0.47 ± 0.07 mM [Student's *t* test, $t(7) = 6.861$, $P < 0.0001$]. However, imposing this increase in $[K^+]_e$ had no detectable effect on the local $[Ca^{2+}]_e$ concentration, suggesting that $[Ca^{2+}]_e$ changes are not secondary to state-dependent $[K^+]_e$ changes [paired *t* test, $t(2) = 0.855$, $P = 0.483$].

Extracellular Mg^{2+} is low during wakefulness and increases during sleep and anesthesia

In sleep and awake states, minor but consistent shifts in free $[Mg^{2+}]_e$ were identified, with $[Mg^{2+}]_e$ decreasing by 0.11 ± 0.01 mM (Fig. 4A) as mice transitioned from sleep to awake and increasing again by 0.13 ± 0.02 mM (Fig. 4B) as animals were observed to return to sleep. Transitions occurred slowly from both sleep to awake (68.9 ± 8.8 s; 5 to 342 s; $n = 55$ transitions) and awake to sleep (141.1 ± 14.8 s; 15.1 to 470 s; $n = 49$ transitions). Isoflurane anesthesia also increased $[Mg^{2+}]_e$ by 0.44 ± 0.07 mM in awake mice (Fig. 4C) before gradually returning to baseline over 26.7 ± 5.7 min (9.6 to 66.3 min, $n = 9$ animals) after the cessation of anesthesia.

Microdialysis samples were collected during the sleep (ZT2 to ZT8) and awake (ZT14 to ZT20) periods and were pooled and compared with isoflurane-induced shifts in $[Mg^{2+}]_e$, demonstrating an increase of 0.32 ± 0.13 mM $[Mg^{2+}]_e$ in isoflurane samples (Fig. 4D). CNQX neither altered basal $[Mg^{2+}]_e$ nor the previously observed isoflurane-induced increase in $[Mg^{2+}]_e$ (Fig. 4E). Thus, across all experiments $[Mg^{2+}]_e$ increased as mice went from awake to sleep or isoflurane (Fig. 4E).

Robust changes in pH were also noted with isoflurane anesthesia. Recordings with pH-sensitive

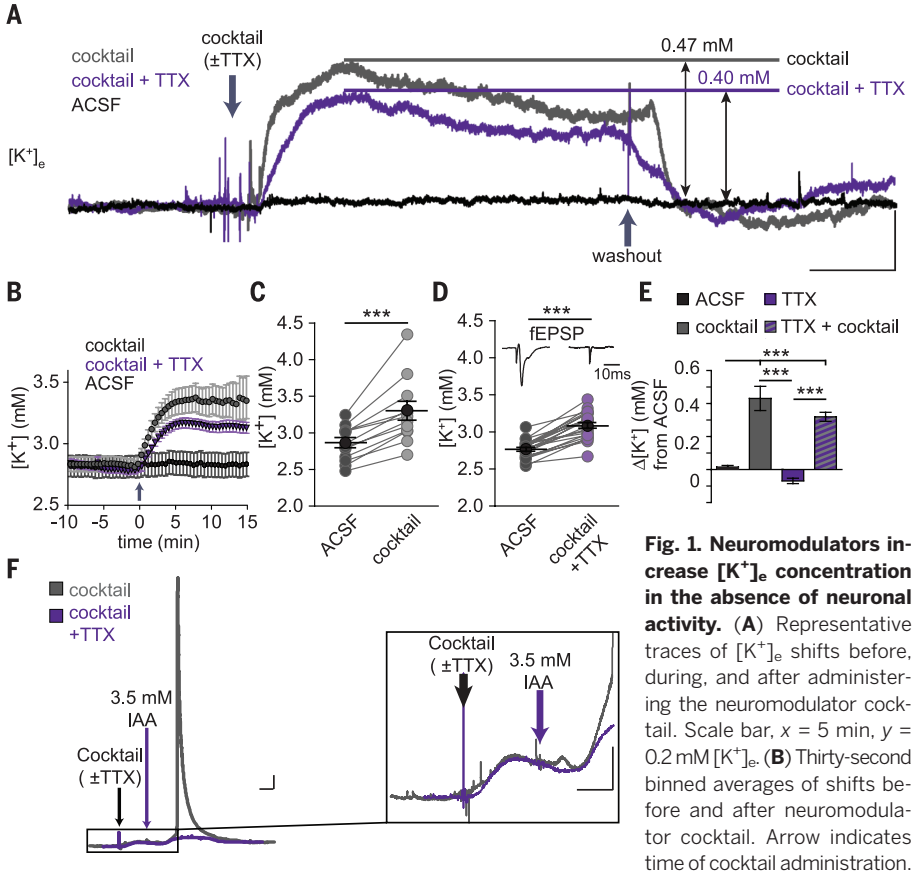

Fig. 1. Neuromodulators increase $[K^+]_e$ concentration in the absence of neuronal activity. (**A**) Representative traces of $[K^+]_e$ shifts before, during, and after administering the neuromodulator cocktail. Scale bar, $x = 5$ min, $y = 0.2$ mM $[K^+]_e$. (**B**) Thirty-second binned averages of shifts before and after neuromodulator cocktail. Arrow indicates time of cocktail administration. (**C** and **D**) Summary of $[K^+]_e$ increase after neuromodulator cocktail application in slices ± TTX [paired *t* test. (C) −TTX, $t(11) = 5.871$, $P = 0.0001$; (D) +TTX, $t(21) = 11.69$, $P < 0.0001$]. (Inset) Representative field excitatory postsynaptic potential (fEPSP) recordings before and after application of TTX. Scale bar, 10 ms. (**E**) Summarized shifts at 10 min after changing perfusion solution. $n = 6$ cocktail-free ACSF, 12 cocktail, 10 ACSF+TTX, and 22 cocktail+TTX slices. One-way analysis of variance (ANOVA), $F(3,46) = 25.94$, $P < 0.0001$. Post-hoc Tukey test, $^{**}P < 0.01$, $^{***}P < 0.001$. (**F**) Representative trace of large $[K^+]_e$ spike after metabolic stress by using iodoacetate (IA). Trace includes pre-cocktail baseline, ACSF + cocktail, ACSF + IA, and return to baseline ACSF. (Right) Magnified trace showing $[K^+]_e$ increases in slices treated with the neuromodulator cocktail (±TTX) followed by IA. Scale bars, $x = 5$ min, $y = 0.2$ mM $[K^+]_e$. Mean (black circle) ± SEM.

microelectrodes showed that pH decreased from an awake level of 7.39 ± 0.03 to a stable isoflurane-anesthetized level of 7.26 ± 0.02 (fig. S3).

Local manipulation of extracellular ions controls neuronal activity and extracellular space volume

Can interstitial ion composition be locally altered to mimic natural sleep or awake concentrations? Because ions in the ACSF covering the cranial window continuously exchange with those in the interstitial fluid, we formulated awake-inducing and sleep-inducing ACSFs (table S1) to drive local cortex to the ionic composition of the state opposite the overarching behavioral state (fig. S4). In sleeping mice (ZT4 to ZT8), the awake-inducing ACSF increased $[K^+]_e$ by 0.47 ± 0.07 mM (versus 0.37 ± 0.06 mM in awake-to-isoflurane transitions), decreased $[Ca^{2+}]_e$ by 0.31 ± 0.06 mM (versus 0.26 ± 0.02 mM), and decreased $[Mg^{2+}]_e$ by 0.35 ± 0.02 mM (versus 0.44 ± 0.07 mM). Sleep-inducing ACSF applied to cortex of awake mice (ZT16 to ZT20) resulted in similar shifts, although in the opposite direction. Thus, both solutions could elicit local changes in $[K^+]_e$, $[Ca^{2+}]_e$, and $[Mg^{2+}]_e$ comparable with those seen in transitions from awake to isoflurane anesthesia (fig. S4, B and D). It was not possible to produce pH shifts of the magnitude seen in awake-to-isoflurane transitions with moderate changes in ACSF pH (~1 pH), likely reflecting the efficacy by which CO_2/HCO_3^- system buffer pH (fig. S4, B and D) (7).

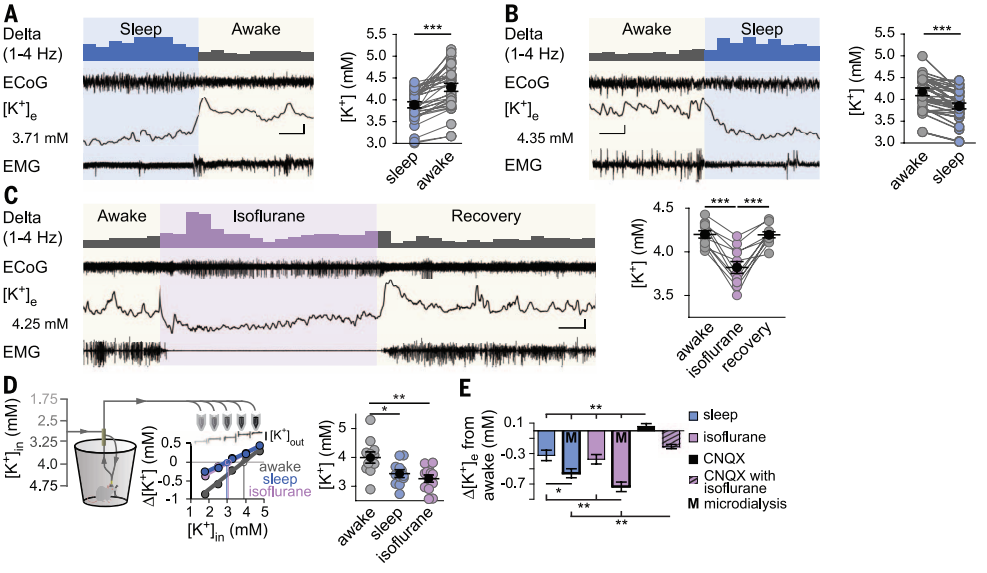

Fig. 2. Extracellular K^+ is higher during wakefulness. (**A** and **B**) Representative ECoG, $[K^+]_e$, and EMG recordings with a data summary of state transitions in (A) sleep-to-awake or (B) awake-to-sleep. Initial $[K^+]_e$ concentrations are shown to the left, and the 1- to 4-Hz power is displayed above so as to illustrate state-dependent shifts, binned at 10 s for clarity. n = 34 transitions; one-way, repeated measures ANOVA, $F(3,99) = 9.536$, $P < 0.0001$. Tukey post-hoc multiple comparisons test, ***$P < 0.001$. Scale bar, x = 20 s, y = 0.1 mM $[K^+]_e$; ECoG = 0.75 mV; EMG = 0.3 mV (A) and 1 mV (B). (**C**) Representative recording of awake-to-isoflurane transitions recorded during the natural awake period (ZT16 to ZT20); n = 11 animals. One-way repeated measures ANOVA, $F(2,20) = 35.61$, $P < 0.0001$. Post-hoc Tukey test, ***$P < 0.001$. Scale bar, x = 1.5 min, y = 0.15 mM $[K^+]_e$, 0.75 mV EMG and ECoG. (**D**) Microdialysis samples collected from freely moving mice during their awake (ZT14 to ZT20) or sleeping (ZT2 to ZT8) period, and under isoflurane anesthesia. (Left) Schematic illustrating setup and inflow $[K^+]$ gradient, with representative ISM trace and sample no-net flux method plot used for $[K^+]_e$ estimate. (Right) Summary of $[K^+]_e$ by state. n = 12 awake, 12 sleep, and 13 isoflurane animals. One-way ANOVA, $F(2,34) = 8.055$, $P = 0.0014$. Post-hoc Tukey test, *$P < 0.05$, **$P < 0.01$. (**E**) Comparison of all state-dependent transitions. One-way ANOVA comparing mean shifts by group, $F(5,161) = 16.61$, $P < 0.0001$. Post-hoc Tukey test, *$P < 0.05$, **$P < 0.01$. Mean (black circle) ± SEM.

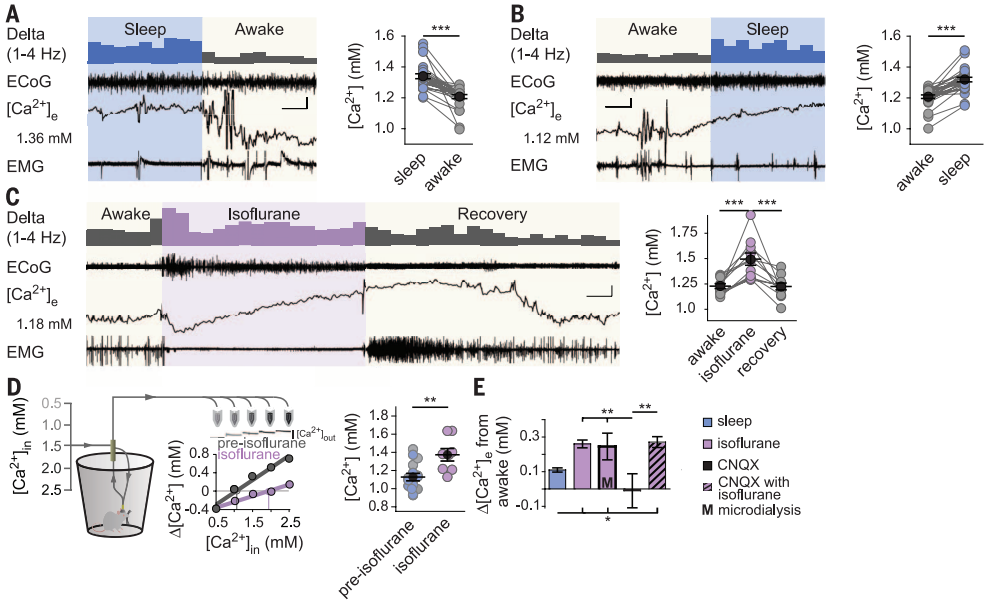

Fig. 3. Extracellular Ca^{2+} decreases during wakefulness. (**A** and **B**) Representative ECoG, EMG, and $[Ca^{2+}]_e$ recordings in (A) sleep-to-awake and (B) awake-to-sleep. Initial $[Ca^{2+}]_e$ is listed to the left with 1- to 4-Hz power presented above. n = 28 transitions. One-way, repeated measures ANOVA, $F(3,81) = 39.91$, $P < 0.0001$. Post-hoc Tukey test, ***$P < 0.001$. Scale bars, x = 20 s (A) and 40 s (B); y, $[Ca^{2+}]_e$ = 0.05 mM, 0.75 mV EMG/ECoG. (**C**) Representative recording of isoflurane induction and recovery (ZT16 to ZT20) and data summary. n = 11 animals. One-way repeated measures ANOVA, $F(2,20) = 18.52$, $P < 0.0001$. Post-hoc Tukey test, ***$P <$ 0.001. Scale bar, x = 6 min, y = $[Ca^{2+}]_e$ = 0.2 mM, 0.5 mV EMG/ECoG. (**D**) Schematic of microdialysis collection. Individual sleep (light blue) and awake (gray) data are pooled and compared with isoflurane. n = 8 awake, 8 sleep, and 8 isoflurane animals. Two-tailed t test of isoflurane versus non-isoflurane, $t(22) = 3.420$, $P = 0.003$, **$P < 0.01$. (**E**) Comparisons of $[Ca^{2+}]_e$ shifts from the awake-to-sleep, isoflurane, CNQX, and CNQX + isoflurane. n = 8 animals; CNQX and CNQX + isoflurane one-way ANOVA comparison of state-dependent shifts, $F(4,117) = 5.824$, $P = 0.0003$; Post-hoc Tukey test, *$P < 0.05$, **$P < 0.01$. Mean (black circle) ± SEM.

Can local manipulation of extracellular ions in itself drive sleep- or awake-like patterns of neuronal activity? We prepared mice with two separate cranial windows located over the left and right hemisphere and recorded ECoG symmetrically from each (Fig. 5A). Starting in sleeping mice (ZT4 to ZT8) with sleep ACSF (table S1) over each window, recordings were collected from each hemisphere. After this baseline period, the ACSF over the left window was removed and replaced with awake-inducing ACSF. When activity in the left hemisphere was normalized to the right in order to preclude changes from global state transitions, we observed a 34 ± 5% decrease in 1- to 4-Hz ECoG power after application of awake-inducing ACSF, with no change in activity in the contralateral hemisphere (Fig. 5B). In comparison, natural sleep-to-wake transitions decrease the 1- to 4-Hz power by 31.1 ± 3.1% (mean ± SEM of all data, n = 128 transitions). Conversely, could sleep-inducing ACSF increase local delta power in awake mice? Recording between ZT16 and ZT20, awake mice were prepared with awake ACSF covering each cranial window. After a baseline recording, the ACSF over the left hemisphere was replaced with sleep-inducing ACSF, resulting in a 43 ± 13% relative increase in 1- to 4-Hz delta power in the left hemisphere exposed to the sleep-inducing ACSF (Fig. 5C).

Because state-dependent changes in brain activity are also linked to marked changes in the extracellular space volume (*10*), we asked whether altering the local ion composition can drive extracellular space volume changes. Tetramethylammonium (TMA^+) recordings showed that in lightly anesthetized mice (1% isoflurane administered so as to avoid arousal episodes), changing ACSF from sleep ACSF to awake-inducing induced a 21.7 ± 1.2% decrease in the local extracellular space volume (Fig. 5D). Tortuosity (λ) was consistent with previous studies (*11*). Conversely, the extracellular space volume increased by 32.2 ± 2.9% from baseline recordings obtained with awake ACSF to those recorded by using sleep-inducing ACSF in awake mice, despite mice remaining awake and mobile, with tortuosity remaining unchanged (Fig. 5D).

Brain-wide manipulations of extracellular ions can override behavioral states

Would global manipulation of the extracellular ion composition be sufficient to change the behavioral state of mice? We implanted EEG and EMG electrodes, as well as a cannula in cisterna magna (*10*). In sleeping mice (ZT4), a baseline recording was acquired by infusing sleep ACSF followed by a switch to a modified awake-inducing ACSF (Fig. 5E). This switch triggered a robust change in EEG/EMG activity (Fig. 5E), with decreased EEG amplitude and delta prevalence and increased EMG activity, indicative of an awake-phenotype. Infusion rates were comparable with CSF production, and ion concentrations were chosen to account for total brain and CSF volume (supplementary materials, materials and methods). Typically, ACSF infusion itself did not alter EEG activity (fig. S5, A and B). Mice returned to sleep shortly after discontinuation of awake-inducing ACSF infusion (Fig. 5F). We next tested whether infusion of a modified sleep-inducing ACSF could alter the behavioral state of mice during their awake-period. Baseline EEG/EMG activity characteristic of awake mice was recorded while infusing awake ACSF followed by a modified sleep-inducing ACSF. Infusion induced a sharp reduction in EMG activity coupled to a marked increase in slow-wave EEG activity, indicating a shift toward sleep. EEG/EMG activity typical of wakefulness rapidly recovered upon stopping infusion of the modified sleep-inducing ACSF (Fig. 5G).

Discussion

Understanding what drives arousal is essential for deciphering key aspects of consciousness and the lack thereof during sleep and anesthesia. We found that the transition from wakefulness to sleep is accompanied by a marked and sustained change in the concentration of key extracellular ions and the volume of the extracellular space. Arousal triggers a rapid rise in $[K^+]_e$, combined with a decrease in $[Ca^{2+}]_e$, $[Mg^{2+}]_e$, and $[H^+]_e$ and a shrinkage of extracellular space. Natural sleep or anesthesia induces the inverse changes in extracellular ion concentrations and is accompanied by an expansion of extracellular space volume. State-dependent shifts in $[K^+]_e$ occurred within seconds, whereas the changes in $[Ca^{2+}]_e$ and $[Mg^{2+}]_e$ were slow, taking 51.5 ± 8.8 s and 68.9 ± 8.8 s, respectively, for sleep-to-awake transitions. Extracellular fluid samples from microdialysis confirmed and extended the in vivo recordings by documenting that state-dependent differences in extracellular $[K^+]_e$, $[Ca^{2+}]_e$, and $[Mg^{2+}]_e$ concentrations persisted over prolonged period of hours in freely behaving animals (Figs. 2 to 4). Microdialysis experiments suggested that state-dependent changes in extracellular ions included

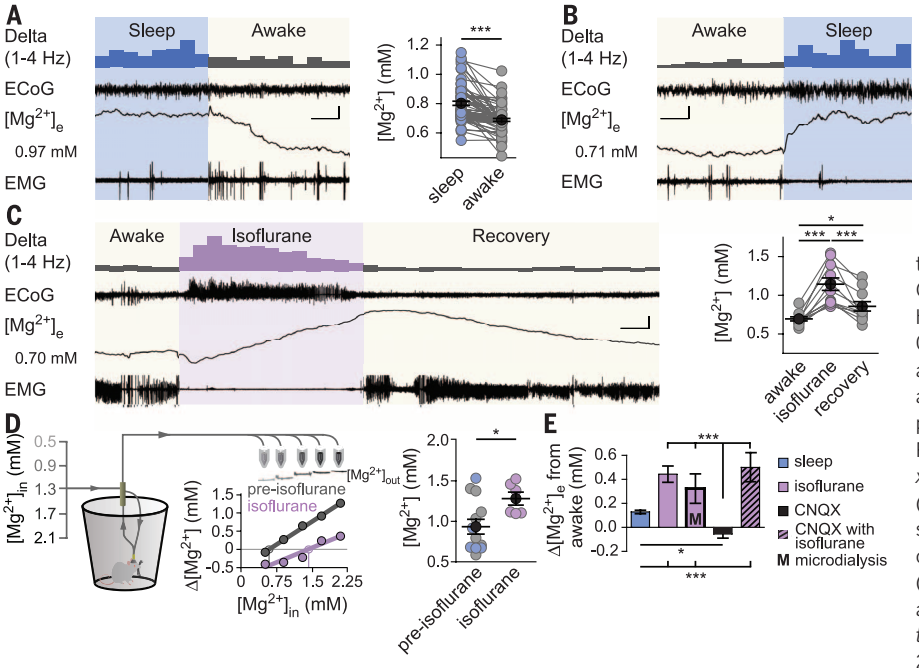

Fig. 4. Extracellular Mg^{2+} decreases during wakefulness. (**A** and **B**) Representative state transitions between sleep and awake ECoG, EMG, and Mg^{2+}-sensitive microelectrodes, with data summary. Initial $[Mg^{2+}]_e$ is given to the left of the ISM trace. n = 73 sleep-to-awake transitions (A) and 58 awake-to-sleep transitions (B). One-way ANOVA, $F(3, 258) = 28.13$, $P < 0.0001$. Post-hoc Tukey test, ***$P < 0.001$. Scale bars, x = 20 s, y = 0.05 mM $[Mg^{2+}]_e$, 0.33 mV EMG/ECoG. (**C**) Representative awake-to-isoflurane recording (ZT16 to ZT20) and summary of changes. n = 11 animals. One-way repeated measures ANOVA, $F(2,20) = 28.13$, $P < 0.0001$. Post-hoc Tukey test, *$P < 0.05$, ***$P < 0.001$. Scale bar, x = 5 min, y = 0.25 mM $[Mg^{2+}]_e$, 0.6 mV EMG/ECoG. (**D**) Schematic of microdialysis collection with data summary. Representative Mg^{2+}-ISM and no-net flux calculation are shown. Sleep (light blue) and awake (gray) are pooled and compared with isoflurane. n = 8 awake, 8 sleep, and 8 isoflurane animals. Two-tailed t test of isoflurane versus pre-isoflurane, $t(16) = 2.427$. $P = 0.0274$ (*$P < 0.05$). (**E**) Comparison of state-dependent $[Mg^{2+}]_e$ shifts from awake-to-sleep, isoflurane, CNQX, and awake + CNQX to isoflurane + CNQX. n = 6 awake-to-CNQX animals and 6 awake + CNQX-to-isoflurane + CNQX animals. One-way ANOVA of relative state-dependent shifts, $F(4,167) = 27.31$, $P < 0.0001$. Post-hoc Tukey test, **$P < 0.01$, ***$P < 0.001$. Mean (black circle) ± SEM.

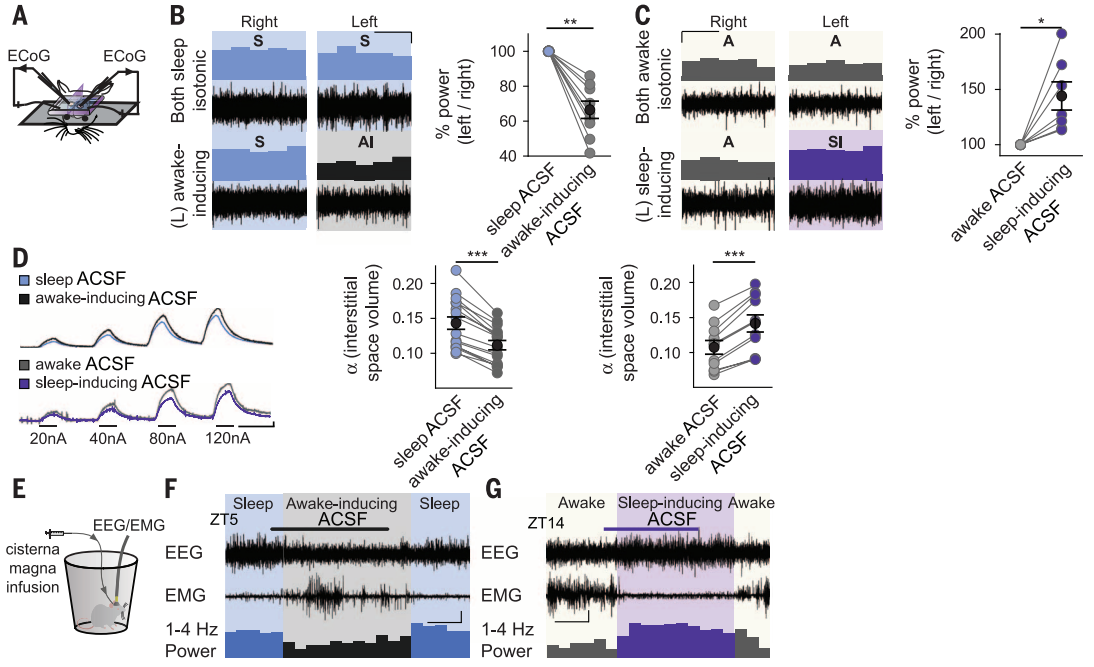

Fig. 5. Imposing changes in extracellular ion concentrations alter local activity, extracellular space, and behavioral state. (**A**) Schematic of double-cranial window recording setup. Symmetrically positioned, separate cranial windows over opposing somatosensory cortices were prepared with ECoGs simultaneously recorded in both hemispheres. (**B** and **C**) Representative ECoG recordings in (B) sleeping (ZT4 to ZT8), and (C) awake (ZT16 to ZT20) mice. (Top) Representative recordings in ACSF mimicking natural state-dependent interstitial ion composition. (Bottom) Recordings after change of left-hemisphere ACSF to (B) awake-inducing or (C) sleep-inducing ACSF. (Right) Summary of 1- to 4-Hz ECoG power shift in the left hemisphere, normalized to the right, after change to (B) awake-inducing or (C) sleep-inducing ACSF. Paired *t* test of 1- to 4-Hz power shifts, (A) $t(8) = 3.530$, $P = 0.008$; (B) $t(6) = 3.091$, $P = 0.0214$. $^{*}P < 0.05$, $^{**}P < 0.01$. Scale bar, $x = 4$ min, $y = 10\%$. (**D**) TMA^{+} traces of shifts in extracellular space volume (α) after switch from sleep to awake-inducing ACSF (top trace) or awake to sleep-inducing ACSF (bottom trace). Higher amplitude equals decreased dilution of TMA^{+} and smaller extracellular space. Data are summarized to the right. Paired *t* test, awake-inducing, $n = 16$ animals; $t(15) = 11.04$, $P < 0.0001$; sleep-inducing, $n = 11$ animals; $t(10) = 8.95$, $P < 0.0001$, $^{**}P < 0.01$. Scale bars, $x = 2$ min, $y = 2$ mV. (**E**) Schematic of cisterna-magna infusion and wire EEG/EMG recording setup. (**F** and **G**) Representative traces showing EEG and EMG activity before, during, and after a 0.3- to 0.5-μl min^{-1} infusion of modified (F) awake-inducing or (G) sleep-inducing ACSF into the cisterna magna. The 1- to 4-Hz relative power (percentage of 1 to 32 Hz) is presented in averaged 10-min bins below. Infusion was run between (F) ZT5.5 and ZT7 (gray bar) and (G) ZT15 and ZT16.5 (purple bar) during sleep and awake periods, respectively. Scale bar, $x = 30$ min, $y = 0.5$ mV (F) and 1mV (G).

widespread cortical areas because the samples were collected by 2-mm-long probes.

All ions exhibited far more consistent, rapid transitions during arousal relative to falling asleep. This is consistent with the need to quickly shift from sleep to awake states when presented with novel, threatening, or unexpected stimuli, and with the overarching ability of brainstem neuromodulatory centers to drive near-immediate responses to behaviorally relevant events (*12*). Relative to $[K^{+}]_e$, the fivefold slower transition of $[Ca^{2+}]_e$ and $[Mg^{2+}]_e$ may reflect differences in the transport or buffering of these ions and suggests that beyond the immediate capacity of neuromodulators to drive quick arousal, it takes longer for composition of interstitial ions to fully stabilize. $[Ca^{2+}]_e$ and $[Mg^{2+}]_e$ exhibited very slow recoveries after anesthesia, often lasting 10 to 30 min. Ions appeared to exhibit larger shifts in the immediate post-induction and recovery period. This biphasic activity may suggest a complex shift in neuromodulatory activity during these anesthetic transitions and, with $[Ca^{2+}]_e$ and $[Mg^{2+}]_e$ taking much longer than $[K^{+}]_e$ to return to a stable awake concentration, may relate to the confusion and postoperative delirium that follows general anesthesia. In fact, high levels of serum $[Ca^{2+}]_e$ and $[Mg^{2+}]_e$ can manifest as subacute delirium (*7*).

Previous studies have shown that $[Mg^{2+}]_e$ in the CNS is in the range of ~0.8 to 1.2 mM or slightly lower than in plasma (*13*, *14*), but $[Mg^{2+}]_e$ homeostasis has received little attention (*15*). In electrophysiological studies, manipulation of $[Mg^{2+}]_e$ is commonly used because low $[Mg^{2+}]_e$ relieves the depolarization block of the *N*-methyl-D-aspartate (NMDA) receptors and facilitates induction of long-term potentiation (LTP) and, in more extreme cases, seizure (*7*, *16*). Wakefulness and sleep deprivation are linked to up-regulation of pathways downstream of NMDA receptor activation, including CamKII, extracellular signal–regulated kinase (ERK), and pCreb (*1*, *17*). The decline in $[Mg^{2+}]_e$ during wakefulness may thereby, in combination with membrane depolarization induced by the elevation of $[K^{+}]_e$, contribute to the gene expression pattern characteristic of wakefulness. The finding that $[Mg^{2+}]_e$ increases during sleep is consistent with the observation that changes in dietary magnesium can have a profound impact on learning and memory, possibly by improving both the amount and quality of sleep (*18*, *19*).

Arousal is triggered by the concerted activity of neurons located in the brainstem, hypothalamus, and basal forebrain (*1*, *4*). Projections from these clusters of neurons release norepinephrine, acetylcholine, orexin, serotonin, dopamine, and histamine over widespread areas of the CNS (*12*). Considerable redundancy exists in the system; acute antagonism, ablation, or activation has documented the importance of the individual components in regulating arousal, but such perturbations rarely produce long-term effects (*12*). An unanswered question is how these neuromodulators drive global changes in EEG activity. Conventional thinking is that the neuromodulators alter the membrane properties and spiking activity of select subtypes of neurons (*5*). Our findings show that a parallel path exists: A cocktail of neuromodulators consistently increased $[K^{+}]_e$ in cortical slices, and TTX did not significantly suppress the $[K^{+}]_e$ increase, suggesting that this shift is not merely a consequence of local synaptic activity. In vivo, inhibition of AMPA receptors only transiently reduced $[K^{+}]_e$, with levels returning to baseline in <10 min despite continued suppression of ECoG activity by >60% (Fig. 2E and fig. S2). This response to an external challenge suggests that ionic homeostasis is tightly regulated in a state-dependent, neuronal activity–independent manner. On the basis of this, we propose that the neuromodulators—in addition to their well-documented, direct effect on neuronal activity—maintain sleep and awake states by creating a state-dependent set-point for interstitial ion concentrations that stabilize over seconds to minutes, minimizing changes that result from transient burst firing or suppression of these brainstem nuclei. In sleep and anesthesia, lower concentrations of $[K^{+}]_e$ will tend to hyperpolarize neurons, with high $[Ca^{2+}]_e$ and $[Mg^{2+}]_e$ enhancing this effect through

surface-charge screening and inactivation of the NALCN channel–dependent Na^+-leak current (*20*). High $[Mg^{2+}]_e$ in combination with hyperpolarization will reduce the likelihood of NMDA receptor activation during sleep, reducing the brain's ability to undergo activity-dependent changes in excitatory transmission (LTP). Manipulation of $[K^+]_e$, $[Ca^{2+}]_e$, and $[Mg^{2+}]_e$ in the CSF bathing the brain drove behavioral shifts between sleep and awake states (Fig. 5). Astrocytic Ca^{2+} signaling is also enhanced by lowering of $[Ca^{2+}]_e$ and $[Mg^{2+}]_e$ (*21*–*23*) and is strongly inhibited by anesthesia (*24*).These observations suggest that regulation of extracellular ion homeostasis is sufficient to alter behavioral state both locally and globally, providing a path for neuromodulators to exert consistent, stable shifts in neuronal and astrocytic activity across the brain.

A myriad of electrophysiological slice studies have in the past taken advantage of minor modifications in the ion composition of the bath solution to induce stable and highly reproducible changes in neural excitability. The observations presented here suggest that the CNS itself uses the same trick to control state-dependent changes in neuronal activity. One advantage of this "ionostatic control" of neural activity is to provide a backdrop for coordinating shifts in behavioral state through the widespread regulation of excitability without relying on complex receptor activation in diverse subclasses of neurons. The characteristic state-dependent pattern of EEG activity can, at least in part, be explained by differences in extracellular ion composition in sleep versus wakefulness. Our observations add new and critical insight into understanding what drives arousal, as well as the loss of consciousness during sleep and anesthesia. Future studies should define whether changes in extracellular ion concentrations are involved in disorders such as stupor and coma.

REFERENCES AND NOTES

1. G. Tononi, C. Cirelli, *Neuron* **81**, 12–34 (2014).
2. J. H. Benington, H. C. Heller, *Prog. Neurobiol.* **45**, 347–360 (1995).
3. V. Hinard *et al.*, *J. Neurosci.* **32**, 12506–12517 (2012).
4. C. B. Saper, T. E. Scammell, J. Lu, *Nature* **437**, 1257–1263 (2005).
5. J. O'Donnell, D. Zeppenfeld, E. McConnell, S. Pena, M. Nedergaard, *Neurochem. Res.* **37**, 2496–2512 (2012).
6. M. Steriade, D. A. McCormick, T. J. Sejnowski, *Science* **262**, 679–685 (1993).
7. G. G. Somjen, *Ions in the Brain: Normal Function, Seizures, and Stroke* (Oxford Univ. Press, 2004).
8. J. Seigneur, D. Kroeger, D. A. Nita, F. Amzica, *Cereb. Cortex* **16**, 655–668 (2006).
9. S. M. Rothman, *Science* **220**, 536–537 (1983).
10. L. Xie *et al.*, *Science* **342**, 373–377 (2013).
11. M. Anděrová *et al.*, *Glia* **35**, 189–203 (2001).
12. C. B. Saper, P. M. Fuller, N. P. Pedersen, J. Lu, T. E. Scammell, *Neuron* **68**, 1023–1042 (2010).
13. A. J. Hansen, *Physiol. Rev.* **65**, 101–148 (1985).
14. L. Sun *et al.*, *Magnes. Res.* **22**, 266–272 (2009).
15. A. M. Romani, *Arch. Biochem. Biophys.* **512**, 1–23 (2011).
16. W. W. Anderson, D. V. Lewis, H. S. Swartzwelder, W. A. Wilson, *Brain Res.* **398**, 215–219 (1986).
17. G. F. Gilestro, G. Tononi, C. Cirelli, *Science* **324**, 109–112 (2009).
18. B. Abbasi *et al.*, *J. Res. Med. Sci.* **17**, 1161–1169 (2012).
19. I. Slutsky *et al.*, *Neuron* **65**, 165–177 (2010).
20. B. Lu *et al.*, *Neuron* **68**, 488–499 (2010).
21. J. Schummers, H. Yu, M. Sur, *Science* **320**, 1638–1643 (2008).
22. H. Sontheimer, *Glia* **11**, 156–172 (1994).
23. A. Torres *et al.*, *Sci. Signal.* **5**, ra8 (2012).
24. A. S. Thrane *et al.*, *Proc. Natl. Acad. Sci. U.S.A.* **109**, 18974–18979 (2012).

ACKNOWLEDGMENTS

This study was supported by NIH (NS078167 and NS078304) and the Office of Naval Research/Department of the Navy. We thank W. Song, R. Rasmussen, E. Nicholas, and W. Peng for expert technical assistance and C. Cirelli, G. Tononi, W. Wang, and C. Nicholson for comments on the manuscript. All authors contributed to data collection, technical design, and writing.

SUPPLEMENTARY MATERIALS

www.sciencemag.org/content/352/6285/550/suppl/DC1
Materials and Methods
Figs. S1 to S5
Table S1
References (*25*–*45*)

18 September 2015; accepted 24 March 2016
10.1126/science.aad4821

REPRODUCTIVE BIOLOGY

Unconventional endocannabinoid signaling governs sperm activation via the sex hormone progesterone

Melissa R. Miller,[1] Nadja Mannowetz,[1] Anthony T. Iavarone,[2] Rojin Safavi,[1] Elena O. Gracheva,[3] James F. Smith,[4] Rose Z. Hill,[1] Diana M. Bautista,[1] Yuriy Kirichok,[5] Polina V. Lishko[1]*

Steroids regulate cell proliferation, tissue development, and cell signaling via two pathways: a nuclear receptor mechanism and genome-independent signaling. Sperm activation, egg maturation, and steroid-induced anesthesia are executed via the latter pathway, the key components of which remain unknown. Here, we present characterization of the human sperm progesterone receptor that is conveyed by the orphan enzyme α/β hydrolase domain–containing protein 2 (ABHD2). We show that ABHD2 is highly expressed in spermatozoa, binds progesterone, and acts as a progesterone-dependent lipid hydrolase by depleting the endocannabinoid 2-arachidonoylglycerol (2AG) from plasma membrane. The 2AG inhibits the sperm calcium channel (CatSper), and its removal leads to calcium influx via CatSper and ensures sperm activation. This study reveals that progesterone-activated endocannabinoid depletion by ABHD2 is a general mechanism by which progesterone exerts its genome-independent action and primes sperm for fertilization.

According to the conventional model of steroid signaling, steroid hormones act through their corresponding genomic receptors to regulate gene expression in development, metabolism, and reproduction (*1*, *2*). The time scale of these signaling events ranges from hours to days (*2*). However, there is a much faster pathway that alters ion channel activity through steroid activation of membrane receptors. Nongenomic signaling of the steroid hormone progesterone (P4) occurs on a time scale of seconds and is required for distinct physiological events, such as oocyte maturation (*3*) and human sperm cell activation (*4*, *5*), and P4 likely triggers anesthesia in rodents (*6*). Many tissues have both nuclear and membrane progesterone receptors, which complicates identification of the latter. Because sperm are transcriptionally silent cells and, therefore, lack the nuclear progesterone receptor effect, we used human spermatozoa as a cellular model to identify the nongenomic progesterone receptor.

Progesterone is a major component of follicular fluid and is released by ovaries and cumulus cells that surround the oocyte. Nanomolar concentrations of P4 act through the nongenomic P4 receptor pathway and cause robust elevation of sperm cytoplasmic $[Ca^{2+}]$ (*7*–*9*) through the activation of the cation channel, CatSper (*10*–*14*). This rise in intracellular $[Ca^{2+}]$ leads to changes in sperm motility, known as hyperactivation, and primes sperm for acrosomal exocytosis (*4*, *5*, *15*). Here, we show that the orphan enzyme α/β hydrolase domain–containing protein 2 (ABHD2) serves as a sperm progesterone receptor. It functions as a lipid hydrolase by removing endogenous CatSper inhibitors upon association with P4. Thus,

[1]Department of Molecular and Cell Biology, University of California, Berkeley, CA 94720, USA. [2]QB3/Chemistry Mass Spectrometry Facility, University of California, Berkeley, CA 94720, USA. [3]Department of Cellular and Molecular Physiology; Department of Neuroscience, Program in Cellular Neuroscience, Neurodegeneration, and Repair (CNNR), Yale School of Medicine, Yale University, New Haven, CT 06536, USA. [4]Department of Urology, University of California, San Francisco, CA 94143, USA. [5]Department of Physiology, University of California, San Francisco, CA 94158, USA.
***Corresponding author. Email: lishko@berkeley.edu**

Changes in the composition of brain interstitial ions control the sleep-wake cycle

Fengfei Ding, John O'Donnell, Qiwu Xu, Ning Kang, Nanna Goldman and Maiken Nedergaard (April 28, 2016)

Science **352** (6285), 550-555. [doi: 10.1126/science.aad4821]

Editor's Summary

Sleep induction through ion changes

How do we switch from sleep to arousal and back? Ding *et al.* found that a combination of modulatory neurotransmitters influenced the levels of extracellular ions in the brain (see the Perspective by Landolt and Holst). This influence was not driven by changes in local neuronal firing, suggesting direct effects of the neuromodulators on extracellular ion composition. However, these changes in interstitial ion levels could switch a brain from wakefulness to sleep. Changes in extracellular ions may thus be a cause, rather than a consequence, of sleep/wake-dependent changes in neuronal activity.

Science, this issue p. 550; see also p. 517

Science (print ISSN 0036-8075; online ISSN 1095-9203) is published weekly, except the last week in December, by the American Association for the Advancement of Science, 1200 New York Avenue NW, Washington, DC 20005.